Int. J. Electrochem. Sci., 13 **(2018)** 1413 – 1422, doi: 10.20964/2018.02.21

International Journal of
ELECTROCHEMICAL
SCIENCE
www.electrochemsci.org

Electrochemical Immune Analysis System for Gastric Cancer Biomarker Carcinoembryonic Antigen (CEA) Detection

Zhenggui Tao, Jinghu Du, Yu Cheng and Qingfeng Li[*]

Xiangyang Central Hospital Affiliated to Hubei University of Arts and Science, Xiangyang, Hubei, 441021, P.R. China
[*]E-mail: liqfeng@hotmail.com

Received: 12 October 2017 / *Accepted:* 23 November 2017 / *Published:* 28 December 2017

In the present work, carcinoembryonic antigen (CEA), a significant biomarker in gastric cancer diagnostics, was successfully detected by a desirably selective and sensitive electrochemical aptasensor with an electrocatalyst and nanocarrier, i.e., Pt/Au-diaminonaphthalene (DN)-graphene. The developed bioconjugate was captured onto the surface of the electrode via a "sandwich" strategy during the detection of CEA. The proposed method was demonstrated to be sensitive, as indicated by the improved electrochemical response, since the dendritic Pt/Au/DN-graphene showed peroxidase-mimic activity for the reduction of H_2O_2 introduced into the electrolytic cell, thereby confirming its desirable catalysis capacity.

Keywords: Sandwich immunosenso; Carcinoembryonic antigen; Biomarker; Electrochemical determination; Pt/Au nanocomposite

1. INTRODUCTION

As one of the most common gastrointestinal cancers around the world, gastric cancer causes millions of patient deaths per year. The survival rate of gastric cancer has been undesirable (20–25%), especially in developing countries [1], which may be a result of late diagnosis to a certain degree. There may be other factors influencing the prognosis of gastric cancer patients apart from tumour-node-metastasis (TNM) stage and choice of treatment, including genetic abnormalities and tumour behaviour and differentiation [2-5]. Thus, the choice of treatment approach is of vital significance for the prognosis of gastric cancer patients. In 1965, carcinoembryonic antigen (CEA), identified by Gold and Freedman [6], was observed to enhance the metastasis of colon carcinoma cells with its sialofucosylated glycoforms which function as selectin ligands [7-9]. CEA is produced in a high proportion of carcinomas in many other organs [9-12]. CEA has a significant effect on the tumour

prognosis due to its influence on tumour metastasis and might be linked with gastric cancer prognosis. Gastric cancer patients show increased CEA levels, which is correlated to patient survival based on a systemic review of serum markers for gastric cancer [13]. According to the literature, preoperative CEA levels could predict the prognosis of gastric cancer [14-17], but several reports present results contradicting this idea [18-23]. There is still controversy surrounding the prognosis of gastric cancer patients with increased CEA levels [24, 25]. Hence, it is essential to develop a state-of-the-art highly specific and sensitive CEA detection method for clinical study and diagnostics.

Electrochemical biosensors are known to be potential tools for sensitive, fast, and accurate health care monitoring at the patient's bedside [26-28]. In an electrochemical biosensor, a transducer system is usually linked to a biological layer via a chemical interface layer, which serves as the interface with the specimen. Therefore, the sensor repeatability, sensitivity, specificity, and stability are influenced by this chemical layer to a large extent. The development of new strategies to prepare electrochemical biosensors has attracted considerable attention. Several examples of favourable biosensors are the following: polyethylene glycol and its derivatives [29], chitosan [30], poly(ethyleneimine) [31], nafion [32], poly(allylamine hydrochloride) [33], and organic thiols [34]. Compared with traditional immunoassays, the antigen–antibody specific reactions based electrochemical immunosensors have attracted considerable attention in recent years because of their measurement precision, instrument simplicity, time-saving analytical procedures, and pretreatment process simplicity. As a result, these sensors have been applied in various fields, including biochemical investigations, clinical diagnosis, and environmental control. Certain signal amplification-based techniques have been used to enhance the biosensor selectivity and sensitivity, especially the use of nanomaterials with remarkable catalytic properties.

The present report describes the fabrication of an electrochemical immunosensor by immobilizing the primary antibody (Ab_1), as well as labelling the secondary antibody (Ab_2) through the formation of a graphene sheet (GS). The Ab_1 was immobilized by adsorbing the selected molecule 1,5-diaminonaphthalene (DN) onto GS through π–π stacking. The GS was subsequently used for coating AuNPs, producing a conjugated complex between Ab_1 and AuNPs. Meanwhile, DN was adsorbed onto GS with the amino group of DN and was later used to coat Pt/Au nanoparticles and conjugate Ab_2 in order to prepare the tracer for Ab_2 labelling. With the use of carcinoembryonic antigen (CEA) as a model analyte, a high-sensitivity immunosensor was prepared using a sandwich strategy.

2. EXPERIMENTS

2.1. Chemicals

Carcinoembryonic antigen (CEA), gold chloride ($HAuCl_4$), toluidine blue (Tb), bovine serum albumin (BSA, 96–99%), chloroplatinic acid (H_2PtCl_6), thrombin (TB), human IgG, and L-cysteine (L-cys) were purchased from Sigma Chemical Co. Polyvinylpyrrolidone (PVP), diaminonaphthalene (DN), ethylenediamine tetraacetic sodium salt (EDTA) and ascorbic acid (AA) were purchased from Chengdu Kelong Chemical Reagent Company (Chengdu, China). Hydrazine hydrate ($N_2H_4{\cdot}H_2O$),

acetone, and ethylene glycol were purchased from Beijing Chemical Reagent Co. (Beijing, China). Sodium tellurite (Na_2TeO_3) was purchased from Aladdin Industrial Corporation. For ELISA analysis, an ELISA kit for CEA determination based on two monoclonal and one polyclonal antibody developed in Immunotech, a Beckman Coulter Company, was used. Format: two-step ELISA 96 wells. Pre-analytical step: extraction in 40% ethanol and centrifugation.

2.2. Preparation of Au/DN-graphene and Pt/Au/DN-graphene nanocomposites

The synthesis of gold nanoparticles was performed according to the method presented in a previous report [35]. After heat treatment to 97 °C, the mixed solution of l mL $HAuCl_4$ (l mL) and 99 mL water was quickly combined with 5 mL trisodium citrate solution (10 g/L) and vigorously stirred. After 10 min of heat treatment of the mixture followed by cooling to room temperature through vigorous stirring, gold colloid was obtained. The synthesis of graphene oxide (GO) was based on a modified Hummer's method [36] followed by reduction of the yielded GO by $NaBH_4$ (reduction agent) for 180 min at 85 °C to yield graphene [37]. DN-graphene was synthesized by homogeneously dispersing 20 mg DN and 60 mg graphene into 60 mL of ethanol–water solution (1:1) under constant stirring for 48 h at 25 °C. The dispersion was later centrifuged and washed three times each with ethanol and water to produce a black powder, which was dried for 24 h at 60 °C under vacuum. This step was followed by vigorous stirring of a mixture of 30 mg DN-graphene nanocomposites and 200 mL AuNPs followed by centrifugation to yield the AuNPs-wrapped DN-graphene, which was thoroughly washed with deionized water thereafter and dried at 60 °C in a vacuum oven for 24 h.

A mixture was obtained by adding 60 mg PVP and 4 mL Au/DN-graphene solution into 30 mL water under magnetic stirring for 10 min. Next, the mixture was quickly injected with 1.6 mL H_2PtCl_6 (1%, w/w) and mixed with 0.1 M AA (2 mL). After the reaction of the above reagents at 60 °C in a water bath for 2 h, a precipitate was formed. The dendritic Pt/Au/DN-graphene was obtained through centrifugation, subjected to repeated washing with distilled water, and dispersed in 3 mL water. The dispersion was then stored at 4 °C in a refrigerator prior to testing.

2.3. Preparation of secondary aptamer bioconjugate

First, 2.5 μM CEA_{apt2} (400 μL) in Tris–HCl buffer (pH 7.4) and 3 mM Tb (100 μL) were injected into 1 mL Pt/Au/DN-graphene solution and stirred below 4 °C overnight. Through this process, thiol-terminated CEA_{apt2} and Tb containing an $–NH_2$ group were attached onto the dendritic Pt/Au/DN-graphene through Pt–S and Pt–N bonding, respectively. Second, the obtained mixture was further mixed with 50 μL BSA (1%, w/w) under 30 min stirring to block the unoccupied active sites of Pt/Au/DN-graphene. After another centrifugation followed suspension in 1 mL water, Pt/Au/DN-graphene–CEA_{apt2}–Tb was yielded as the resulting bioconjugate. For these tests, the reaction temperature was set at 4 °C. For comparison, the preparation of Au/DN-graphene–CEA_{apt2}–Tb bioconjugate without Pt was performed via comparable procedures.

2.4. Fabrication of the immunosensor and electrochemical sensing procedure

The bare GCE was carefully and successively polished with Al_2O_3 powder (0.3 μm and 0.05 μm), followed by ultrasonication in ethanol and doubly distilled water. Gold nanoparticles (AuNPs) were later electrodeposited on the obtained GCE 1% w/w $HAuCl_4$ solution at a potential of −0.2 V for 30 s. This step was followed by dropping 20 μL CEA_{apt1} (2.5 μM) in Tris–HCl buffer (pH 7.4) onto the coated GCE surface for 18 h at room temperature, which led to the successful immobilization of CEA_{apt1} through Au–S affinity. To block the residual active sites, as well as eliminating the non-specific binding effects, the resulting GCE was incubated for 40 min in 20 μL BSA (1%, w/w). Subsequently, the resulting GCE was modified by adding 20 μL CEA standard solution at given concentrations for 40 min at room temperature. This step was followed by incubation of 20 μL Pt/Au/DN-graphene–CEA_{apt2}–Tb for another 1 h. After rinsing with distilled water, the obtained sandwich-type aptasensor was stored at 4 °C prior to testing. A multi-impedance test configuration was used for the electrochemical impedance spectroscopy (EIS) analysis, in which the AC amplitude was 10 mV, and the frequency ranged from 10 kHz to 10 mHz. Cyclic voltammetry (CV) was performed at a scan rate of 50 mV/s, and the potential range was -0.2-0.6 V. Differential pulse voltammetry (DPV) measurement was also performed, where the step potential and pulse amplitude were 2 mV and 50 mV, respectively, and a 50 ms pulse, a scan rate of 15 mV/s, a sampling time of 10 ms, and a 100 ms pulse interval were applied.

3. RESULTS AND DISCUSSION

Fig. 1 shows the CVs recorded for the preparation of the developed aptasensor in 5 mM $K_3[Fe(CN)_6]/K_4[Fe(CN)_6]$ with a scan rate of 50 mV/s. For the unmodified GCE, the CV curve was reversible. However, after the $HAuCl_4$ (1%, w/w) was electrodeposited, an increase in peak current was observed, since the charge transfer was enhanced by the conductivity of nano-Au. The peak current decreased after CEA_{apt1} was immobilized, indicating hindrance of the charge transfer channel by the CEA_{apt1}. A further decrease in the electrochemical response was observed upon immobilization of the non-conductive BSA to the surface of the final GCE. Another decrease in the peak current was observed after 10 ng/mL CEA was added. This finding suggests that the complex CEA_{apt1}–CEA was formed on the surface of the final GCE, causing the formation of an inert blocking layer, which hindered the charge transfer. The transport of $[Fe(CN)_6]^{4-/3-}$ towards the surface of the electrode was subsequently hindered by the formed immunocomplex, which acted as an inert blocking layer [38].

To further study the interface features of the coated GCE, electrochemical impedance spectroscopy (EIS) experiments were also conducted. For the bare GCE, an extremely small semicircle region was recorded, as shown in Fig. 1B. However, a smaller semicircle region was recorded after the 1% $HAuCl_4$ (w/w) was electrodeposited, which indicated that the nano-Au was perfectly conductive. Conversely, after CEA_{apt1} was immobilized, a significant increase in semicircle diameter was observed, suggesting blocking of the charge transfer tunnel by the CEA_{apt1}. The semicircle diameter further increased after the residual active sites were blocked by the inserted BSA, which indicated that the charge transfer was also hindered by BSA. This response was observed to decrease with the

immobilization of anti-CEA on the surface of the electrode as a result of the production of anti-CEA/CEA immunocomplex. Another increment in the diameter of the semicircle was observed after incubating the final aptasensor with CEA (10 ng/mL), since a complex of CEA_{apt1}–CEA was formed and blocked the charge transfer tunnel.

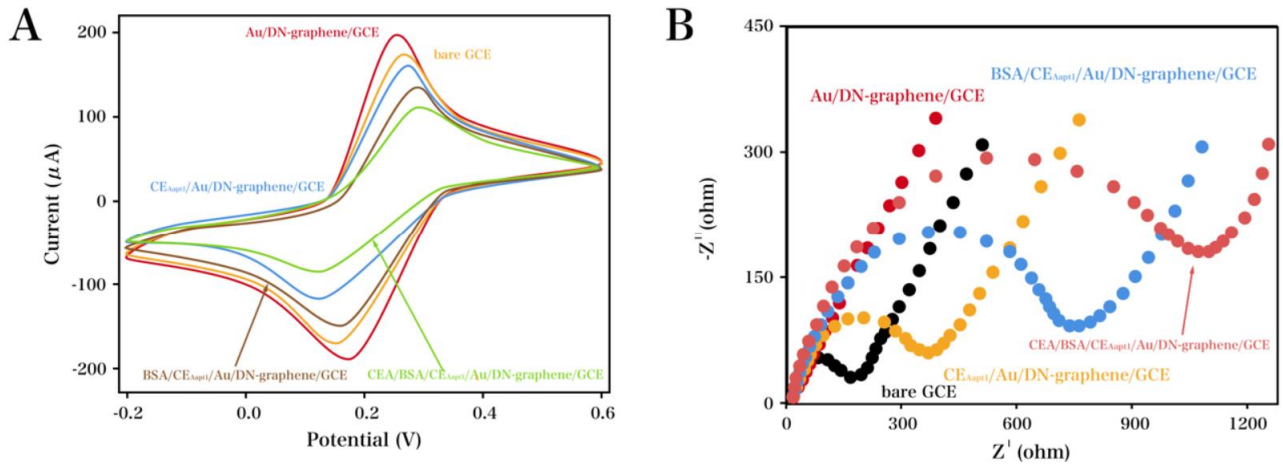

Figure 1. (A) CVs and (B) EIS patterns recorded for the electrode coated step-wise in 5 mM $K_3[Fe(CN)_6]/K_4[Fe(CN)_6]$, CV scan rate was 50 mV/s (CEA (10 ng/mL) and CEA_{apt1} (2.5 μM) incubated for 40 min).

A performance comparison of the two secondary aptamer bioconjugates, Au/DN-graphene–CE_{Aapt2}–Tb and Pt/Au/ND-graphene–CEA_{apt2}–Tb, under the optimum parameters was performed to study the catalytic capacity of Pt/Au/DN-graphene in the developed bioconjugate. Upon the immobilization of 10 ng/mL CEA onto Au/ND-graphene–CEA_{apt2}–Tb, only a slight increase in DPV response was observed after adding H_2O_2 (0.8 mM) into the PBS (1 mL), as displayed in Fig. 3A.

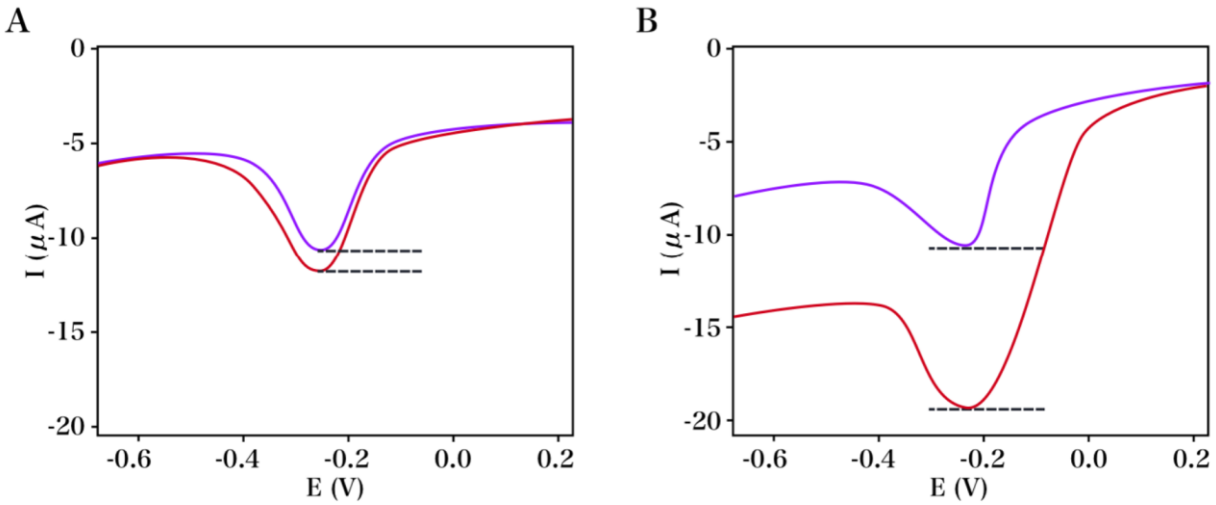

Figure 2. DPVs recorded for the aptasensor after incubation with CEA (10 ng/mL), CEA_{apt1} (2.5 μM), and the following two secondary aptamer bioconjugates: (A) Au/ND-graphene–CEA_{apt2}–Tb; (B) Pt/Au/ND-graphene-CEA_{apt2}–Tb, in pH 7.0 PBS (1 mL, 0.1 M) before and after adding 0.8 mM H_2O_2.

However, both before and after the addition of H_2O_2 (0.8 mM) into the PBS (1 mL), the DPV response was drastically increased after the developed bioconjugate Pt/Au/ND-graphene–CEA_{apt2}–Tb was used on the GCE surface, as shown in Fig. 2B. The Pt/Au/ND-graphene was highly catalytic, which suggested that the developed bioconjugate possessed more than nine times the electrochemical amplification capacity. Pt/Au/ND-graphene was also highly catalytic to the reduction of H_2O_2, facilitating the charge transfer of Tb and increasing the electrochemical response. These results confirmed that the developed aptasensor has the potential to be highly sensitive and could be used as a remarkable analytical tool for the preparation of a desirable platform for the determination of CEA.

The potential for the use of the Pt/Au/ND-graphene-based aptasensor toward the detection and quantitative analysis of CEA was studied under optimum parameters by recording the electrochemical response in PBS (1 mL) that contained H_2O_2 (0.8 mM). The aptasensor after incubation with CEA at varying concentrations was also characterized via DPVs, as shown in Fig. 3A, along with the corresponding calibration plot of DPV peak current relative to the CEA concentration. In brief, as the concentration of CEA was increased from 0.001 to 80 ng/mL, an increase in current response was observed, since the Pt/Au/ND-graphene–CEA_{apt2}–Tb bioconjugate was developed via the specific sandwich-type reaction between CEA_{apt2} and CEA due to the increased amount of CEA on the GCE surface. The DPV signal was also found to be linearly related to the logarithm of CEA concentration. The limit of detection (LOD) of the developed sensor was 0.007 pM, as determined based on a literature reference [39]. Fig. 3B shows the calibration plot recorded for the DPV peak current in the presence of CEA with only the Au/ND-graphene amplification. The sensitivity and dynamic linear range of Au/ND-graphene were both less desirable than those of dendritic Pt/Au/ND-graphene, due to the more favourable electrocatalytic activity of the dendritic Pt/Au/ND-graphene to H_2O_2 reduction, as well as its more significant amplification capacity for the electrochemical response. Table 1 shows the performance comparison of our proposed sensor with others previously reported in the literature.

Table 1. Comparison of proposed CEA immunosensor with previous reports.

Immunosensor	Detection range (ng/mL)	Limit of detection (ng/mL)	Reference
Thiourea modified gold electrode	0.01-10	0.01	[40]
Conducting long-chain polythiols	0.00001-10	0.0000015	[41]
Graphene-nafion	0.5-120	0.17	[42]
MWCNT-NH_2-PdPt nanocages	0.001-20	0.0002	[43]
Pt/Au/ND-graphene–CEA_{apt2}–Tb	0.001 to 20	0.0007	This work

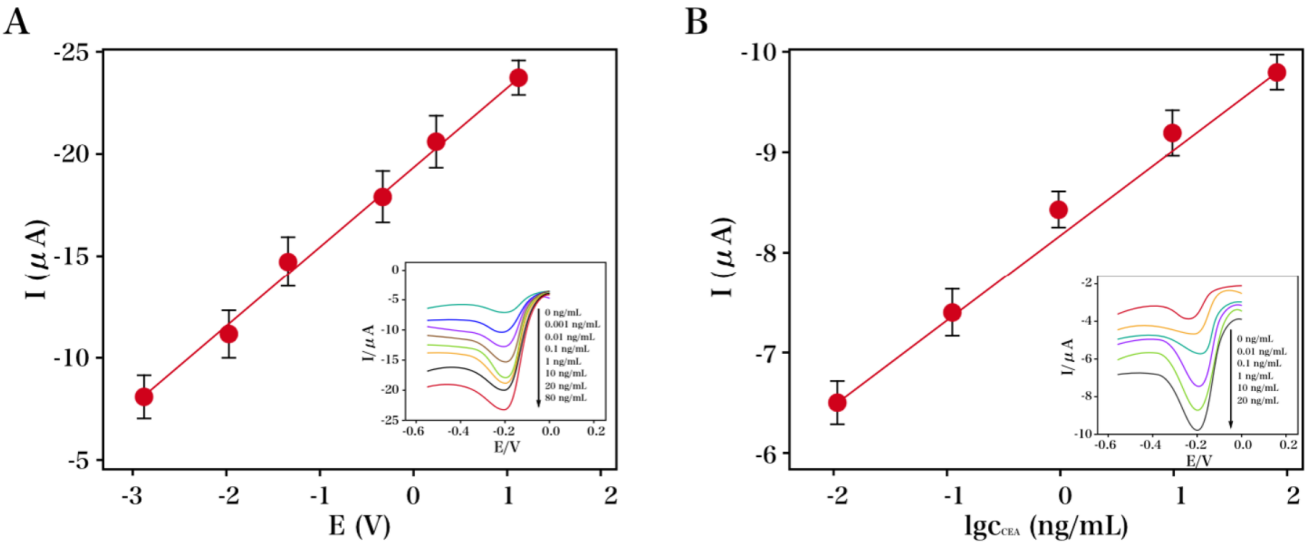

Figure 3. Calibration plot of the DPV peak current relative to CEA concentrations with two secondary aptamer bioconjugates: (A) Pt/Au/ND-graphene–CEA$_{apt2}$–Tb; (B) Au/ND-graphene–CEA$_{apt2}$–Tb. Insets: DPV responses recorded for our developed aptasensor towards varying CEA concentrations.

The electrochemical responses of some interfering agents, including L-cys, thrombin (TB), human IgG, and alpha fetoprotein (AFP) in 1 mL PBS that contained 0.8 mM H_2O_2 were recorded to study the specificity of the developed aptasensor. In the presence of 100 ng/mL human IgG, L-cys, TB and AFP, no significant DPV signal was recorded, as indicated in Fig. 4. Conversely, the presence of the target CEA (10 ng/mL) and its mixture with these interfering agents (100 ng/mL) led to a significant DPV response signal. The Pt/Au/ND-graphene–CEA$_{apt2}$–Tb bioconjugate-based sensor was desirably specific, since the Pt/Au/ND-graphene was highly catalytic and could remarkably amplify the electrochemical response. These results demonstrated that the application of this immunosensor in the detection of CEA in serum samples is very promising.

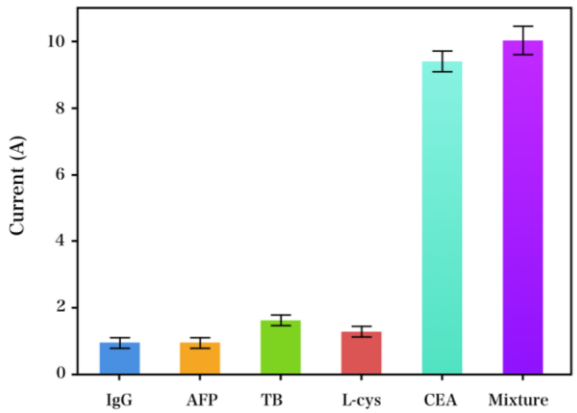

Figure 4. Study on the specificity of our developed aptasensor to 10 ng/mL target CEA in the presence of different interfering agents, including L-cys, TB, AFP, IgG, and their mixture with 10 ng/mL CEA.

Under comparable parameters, the electrochemical responses of four prepared aptasensors after incubation with CEA at the same concentration of 10 ng/mL were recorded to study the reproducibility of our developed aptasensor. The electrochemical signal was found to be reproducible, and the relative standard deviation (RSD) was 5.1%, which suggested that our developed method meets the desired level of reproducibility. The aptasensor was stored at 4 °C for 10 d, and its DPV responses to the CEA (10 ng/mL) in 1.07 mL PBS that contained 0.8 mM H_2O_2 were subsequently recorded to study the aptasensor stability. According to the results, the peak current of DPV retained 94.4% of the original current, which suggests that our developed aptasensor was highly stable for the detection of CEA. This result is comparable with those obtained for several previously reported sensors, such as conducting long-chain polythiol-constructed immunosensors and graphene-nafion composite-constructed immunosensors [41, 42].

Table 2 shows the results and relative deviations obtained using both immunosensors and ELISA analysis. The relative errors between the two techniques ranged from 3.81% to 7.77%, indicating that the results obtained from the immunosensors was acceptably close to those obtained by ELISA. Therefore, accurate determination of CEA in clinical diagnosis by as-prepared immunosensors was achieved with satisfactory results.

Table 2. Experimental results of CEA concentration in serum samples obtained by immunosensors and ELISA techniques.

Serum samples	1	2	3
Proposed Immunosensor (ng/mL)	0.52	5.15	10.51
Added (ng/mL)	2	2	2
Found (ng/mL)	2.51	7.13	12.48
Recovery (%)	99.60	99.72	99.76
Relative deviation (%)	7.77	3.81	6.45
ELISA (ng/mL)	0.51	5.12	10.27

4. CONCLUSIONS

In this report, a sandwich-type aptasensor fabricated based on a Pt/Au/ND-graphene–CEA_{apt2}–Tb bioconjugate provided a selective and sensitive analysis of CEA. The charge transfer and the electrochemical response signal were promoted through catalysis of the reduction of H_2O_2 introduced into the electrolyte cell, since dendritic Pt/Au/ND-graphene is highly conductive and possesses peroxidase-mimic activity. Therefore, our developed aptasensor was observed to promote analytical capacity and to achieve desirable sensitivity.

References

1. J. Gao, Z. Guo, F. Su, L. Gao, X. Pang, W. Cao, B. Du and Q. Wei, *Biosensors & Bioelectronics*, 63 (2015) 465.
2. G. J, G. Z, S. F, G. L, P. X, C. W, D. B and W. Q, *Biosensors & Bioelectronics*, 63C (2015) 465.

3. Z. Si, B. Xie, Z. Chen, C. Tang, T. Li and M. Yang, *Microchimica Acta*, (2017) 1.
4. N. Li, Y. Wang, W. Cao, Y. Zhang, T. Yan, B. Du and Q. Wei, *Journal of Materials Chemistry B*, 3 (2015) 2006.
5. Z. Mu, L. Jiao, Q. Wei and H. Li, *Rsc Advances*, 6 (2016) 42994.
6. P. Gold and S.O. Freedman, *Journal of Experimental Medicine*, 121 (1965) 439.
7. G. Alexander, C. Nielsen, S. Dan-Tiberiu, I. Sahika, D. Mary, M. Niazi, D. Hanifi, A. Aram, G. Malliaras and R. Jonathan, *Nature Communications*, 7 (2016) 13066.
8. C.B. Nielsen, G. Alexander, S. Dan-Tiberiu, B. Enrico, M. Niazi, D. Hanifi, S. Michele, A. Aram, G. Malliaras and R. Jonathan, *Journal of the American Chemical Society*, 138 (2016) 10252.
9. L. Tian, L. Liu, Y. Li, Q. Wei and W. Cao, *Scientific Reports*, 6 (2016) 30849.
10. H. Quan, C. Zuo, T. Li, Y. Liu, M. Li, M. Zhong, Y. Zhang, H. Qi and M. Yang, *Electrochimica Acta*, 176 (2015) 893.
11. N. Anh, H. Trung, B. Tien, N. Binh, H. Cao, N. Huy, N. Loc, V. Thu and T. Lam, *Journal of Electronic Materials*, 45 (2016) 2455.
12. S. Staden, I. Comnea-Stancu and C. Surdu-Bob, *Journal of the Electrochemical Society*, 164 (2017) B267.
13. L. Gugoasa, S. Staden, A. Al-Ogaidi, C. Stanciu-Gavan, J. Staden, M. Rosu and S. Pruneanu, *Journal of the Electrochemical Society*, 164 (2017) B443.
14. T. Xu, X. Li, Z. Xie, X. Li and H. Zhang, *Microchimica Acta*, 182 (2015) 2541.
15. B. Roux, C. Bourbon, J. Colin and V. Pralong, *Rsc Advances*, 5 (2015) 72801.
16. J. Li, H. Xie, Y. Liu, R. Hang, W. Zhao and X. Huang, *Talanta*, 144 (2015) 404.
17. J. Liu, J. Wang, T. Wang, D. Li, F. Xi, J. Wang and E. Wang, *Biosensors & Bioelectronics*, 65 (2015) 281.
18. D. Wang, G. Ning, H. Zhang, T. Li, Q. Li, Y. Cao, X. Su and S. Jiang, *Biosensors & Bioelectronics*, 65 (2015) 78.
19. Z. Wang, N. Liu, F. Feng and Z. Ma, *Biosensors & Bioelectronics*, 70 (2015) 98.
20. D. Feng, L. Li, J. Zhao and Y. Zhang, *Analytical Biochemistry*, 482 (2015) 48.
21. Y. Wang, H. Xu, J. Luo, J. Liu, L. Wang, Y. Fan, S. Yan, Y. Yang and X. Cai, *Biosensors & Bioelectronics*, 83 (2016) 319.
22. Z. Liu, Q. Rong, Z. Ma and H. Han, *Biosensors & Bioelectronics*, 65 (2015) 307.
23. Y. Gao, X. Zhu, J. Xu, L. Lu, W. Wang, T. Yang, H.K. Xing and Y.F. Yu, *Analytical Biochemistry*, 500 (2016) 80.
24. W. Lu, T. Lin, Y. Wang, X. Cao, J. Ge, J. Dong and W. Qian, *Ionics*, 21 (2015) 1141.
25. Z. Liu, Y. Wang, Y. Guo and C. Dong, *Electroanalysis*, 28 (2015) 1023.
26. X. Cai, S. Weng, R. Guo, L. Lin, C. Wei, Z. Zheng, Z. Huang and X. Lin, *Biosensors & Bioelectronics*, 81 (2016) 173.
27. J. Zhao, Z. Guo, J. Guo, J. Wang and Y. Zhang, *Rsc Advances*, 6 (2016) 31448.
28. D. Ortiz, I. Gordon, S. Legand, V. Dauvois, J. Baltaze, J. Marignier, J. Martin, J. Belloni, M. Mostafavi and S.L. Caër, *Journal of Power Sources*, 326 (2016) 285.
29. M. Chen, C. Zhao, Q. Xu, B. Nie, L. Xu, S. Weng and X. Lin, *Analytical Methods*, 7 (2015) 10339.
30. T. Feng, X. Qiao, H. Wang, Z. Sun, Y. Qi and C. Hong, *Journal of Materials Chemistry B*, 4 (2016) 990.
31. S. Samanman, A. Numnuam, W. Limbut, P. Kanatharana and P. Thavarungkul, *Analytica Chimica Acta*, 853 (2015) 521.
32. Y. Yu, Q. Zhang, J. Buscaglia, C. Chang, Y. Liu, Z. Yang, Y. Guo, Y. Wang, K. Levon and M. Rafailovich, *Analyst*, 141 (2016) 4424.
33. R. Wallen, N. Gokarn, P. Bercea, E. Grzincic and K. Bandyopadhyay, *Nanoscale Research Letters*, 10 (2015) 268.
34. C. Hébert, E. Scorsone, M. Mermoux and P. Bergonzo, *Carbon*, 90 (2015) 102.
35. P. Tartaj, T. González-Carreño and C. Serna, *Langmuir*, 18 (2002) 4556.

36. R. Muszynski, B. Seger and P. Kamat, *J Phys Chem C*, 112 (2008) 5263.
37. Y. Zhao, L. Zhan, J. Tian, S. Nie and Z. Ning, *Electrochimica Acta*, 56 (2011) 1967.
38. X. Li, X. Zhang, Z. Wang, Q. Zhang, W. Xuan and L. Ma, *Int. J. Electrochem. Sc.*, 11 (2016) 10020.
39. A. Radi, J. Acero Sánchez, E. Baldrich and C. O'Sullivan, *Journal of the American Chemical Society*, 128 (2006) 117.
40. V. Salgueiriño-Maceira, M. Correa-Duarte, M. Farle, A. López-Quintela, K. Sieradzki and R. Diaz, *Chemistry of Materials*, 18 (2006) 2701.
41. Y. Arntz, J. Seelig, H. Lang, J. Zhang, P. Hunziker, J. Ramseyer, E. Meyer, M. Hegner and C. Gerber, *Nanotechnology*, 14 (2002) 86.
42. Y. Li, W. Yang, M. Fan and A. Liu, *Analytical Sciences*, 27 (2011) 727.
43. N. Li, Y. Wang, W. Cao, Y. Zhang, T. Yan, B. Du and Q. Wei, *Journal of Materials Chemistry B*, 3 (2015) 2006